Supplemental Materials and Methods.

Cells. Primary fibroblasts were obtained through the culture of the patient's skin biopsy and further transformed by transfection with SV40 large T expression plasmids. Control primary fibroblasts were from age-matched healthy donors. Cernunnos-deficient cells were described previously [1]. Fanconi anemia fibroblasts were from a FANCG-mutated patient described in Lesport et al. [2]. Bloom-deficient fibroblasts were kindly provided by Yanick Crow [3] (Imagine Institute, Paris, France). When indicated the SV40-fibroblasts were immortalized by transduction with the hTERT-expressing lentiviral vector pLV-hTERT-IRES-hygro (a gift from Tobias Meyer; Addgene plasmid #85140).

Telomere length measurement by fluorescence *in situ* hybridization and flow cytometry (Flow-FISH). The average length of telomere repeats at chromosome ends in individual PBMCs was measured by Flow-FISH using fluorescein isothiocyanate (FITC)-conjugated $(CCCTAA)_3$ peptide nucleic acid probe (DakoCytomation, Glostrup, Denmark) on a BD FACS Canto II (BD Bioscience). Calculation of relative telomere length of the patient's isolated PBMCs was performed by comparing the fluorescence of these cells with the tetraploid 1301 cell line (Sigma-Aldrich), a tetraploid ALL-T cell line with long telomeres, and expressed as a percentage. Samples were analyzed in triplicate when enough cells were available. Values from 543 healthy individuals (ranging from 10 days to 77 years old) were used to determine the distribution of age-dependent relative telomere lengths. Very short telomeres were defined as a telomere length below the 1st percentile of the normal relative telomere length distribution.

Telomere restricion fragment analysis (TRF). Genomic DNA (800ng) extracted from cells was digested with HinfI and RsaI enzymes, resolved by a 0.7 % agarose gel, and transferred to a nylon membrane. Hybridization was performed overnight at 42 °C using EasyHyb solution (Roche) and γ-^{32}P-labeled $(TTAGGG)_4$ probe. After washes, membranes were exposed over a PhosphorImager (AGFA). PhosphorImager exposures of telomere-probed Southern blots were analyzed with the ImageJ program. The digitalized signal data were then transferred to Microsoft Excel and served as the basis for calculating mean TRF length using the formula L = (ODi)/(ODi/Li), where ODi = integrated signal intensity at position i and Li = length of DNA fragment in position i.

Whole exome sequencing. Exome capture was performed using the SureSelect Human All Exon kit (Agilent Technologies®, Santa Clara, CA). Agilent SureSelect Human All Exon (54 Mb, Clinical research Exome) libraries were prepared from 3 µg of genomic DNA sheared with an Ultrasonicator (Covaris®, Woburn, MA) as recommended by the manufacturer. Barcoded exome libraries were pooled and sequenced using a HiSeq2500 (Illumina®, San Diego, CA), generating 130x130 paired-end reads. After demultiplexing, sequences were mapped on the human genome reference (NCBI build37/hg19 version) with BWA. The mean depth of coverage obtained of the exome library was 138 X with >99 % of the targeted exonic bases covered at least by 15 independent reads and >97 % by at least 30 independent sequencing reads (>99 % at 15 X and >99 % at 30 X). Variant calling was

carried out with the Genome Analysis Toolkit (GATK), SAMtools and Picard Tools. Single nucleotide variants were called with GATK Unified Genotyper, whereas indel calls were made with the GATK IndelGenotyper_v2. All variants with a read coverage ≤ 2x and a Phred-scaled quality of ≤ 20 were filtered out. All the variants were annotated and filtered using PolyWeb, an in-house developed annotation software. The initiation codon is codon 1.

Targeted sequencing of telomere genes. Complete sequencing of the coding region and flanking intronic regions (± 8 bp) of *ACD* genes (NM_001082486.1; chr.16), *DCLRE1B* (NM_022836.3; chr.1), *DKC1* (NM_001363.4,chr.X), *NHP2* (NM_017838.3; chr.5), *NOP10* (NM_018648.3; chr.15), *PARN* (NM_002582.3;chr.16), *RTEL1* (NM_032957.4; chr.20), *TERC* (NR_001566.1; chr.3), *TERT* (NM_198253.2;chr.5), *TINF2* (NM_001099274.1; chr.14) was done as follow. Targeted regions were captured by using probe oligonucleotides (QXT, Agilent Technologies) and sequenced by next-generation sequencing (MiSeq, Illumina, Inc). Alignment and identification of the bases were carried out through Burrows-Wheeler Aligner (BWA-MEM) and Genome Analysis Toolkit (GATK).

Telomere Shortest Length Assay (TeSLA). TeSLA was performed essentially as described by Lai et al. [4]. Briefly, an equimolar mixture (50 pM each) of the six TeSLA-T oligonucleotides (containing seven nucleotides of telomeric C-rich repeats at the 3′ end and 22 nucleotides of the unique sequence at the 5’ end) was annealed to and ligated with 50 ng of undigested genomic DNA at 35 °C for 14 h. Then, genomic DNA was digested with *Cvi*AII, *Bfa*I, *Nde*I, and *Mse*I, the restriction enzymes that create short either AT or TA overhangs. Digested DNA was then treated with Shrimp Alkaline Phosphatase to remove 5′ phosphate from the DNA fragments to avoid their ligation to each other during the subsequent step. Upon heat-inactivation of phosphatase, partially double-stranded AT and TA adapters were added (final concentration 1 μM each) and ligated to the dephosphorylated fragments of genomic DNA at 16 °C overnight. Following ligation of the adapters, genomic DNA was diluted to a final concentration of 20 pg/μL, and 2-4 μL of it was used in a 25 μL PCR reaction to amplify terminal fragments using primers complementary to the unique sequences at the 5’ ends of the TeSLA-T oligonucleotides and the AT/TA adapters. FailSafe polymerase mix (Epicenter) with 1× FailSafe buffer H was used to efficiently amplify G-rich telomeric sequences. Entire PCR reactions were then loaded onto the 0.9 % agarose gel for separation of the amplified fragments. To specifically visualize telomeric fragments, the DNA was transferred from the gel onto the nylon membrane by Southern blotting procedure and hybridized with the ^{32}P-labeled $(CCCTAA)_3$ probe. The sizes of the telomeric fragments were quantified using TeSLA Quant software [4].

Telomeric FISH. Seeded cells were arrested in metaphase with 60 ng/mL colcemid (KaryoMAX, Invitrogen) for 1 h, harvested, and resuspended in 75 mM KCl for 15 min at 37 °C. Cells were then fixed in 3:1 (v:v) methanol/acetic acid and dropped onto glass slides. Metaphase spreads were fixed in 4 % formaldehyde in PBS for 2 min and dehydrated with sequential immersions into 50, 70, and 100 % ethanol baths for 2 min each and then air-dried. Telomere PNA-FISH was performed in 70 % deionized formamide, 1 % blocking reagent (Roche), and 0.3 μg/mL Cy3-$(CCCTAA)_3$ PNA probe (Panagene). DNA was denatured for 5 min at 80 °C, then hybridized for 2 h at room temperature (RT).

Slides were next washed as follows: 2 × 15 min at RT in 70 % formamide, 10 mM Tris pH 7.2 and 3 × 5 min in 50 mM Tris pH 7.5, 150 mM NaCl, and 0.05 % Tween-20. Slides were then dehydrated in ethanol, air-dried, and counterstained with DAPI mounted in Vectashield (Vector Laboratories). National Institutes of Health software (ImageJ) was used for the quantitative analysis of images.

Detection of TIF and β-galactosidase activity. For telomere dysfunction-induced foci (TIF) analysis, cells grown on coverslips were fixed with 2 % paraformaldehyde for 10 min, permeabilized with 0.1 % Triton X-100 for 30 min, and incubated with anti-53BP1 (Novus Biological NB100-304; RRID: AB_10003037**;** 1:200) for 1h at RT. After washing and incubation with the secondary antibody, cells were washed in PBS and dehydrated in sequential ethanol baths, and FISH was performed as described above. For senescence-associated β-galactosidase staining, primary fibroblasts were fixed at room temperature for 10 min in 4 % paraformaldehyde in PBS, washed in PBS, and then stained in β-galactosidase fixative solution (Senescence β-Galactosidase Staining Kit, # 9860, Cell Signaling) at 37 °C for 16 h before cell imaging.

In-gel G-overhang assay. In-gel G-overhang assay was performed as described [5], with minor modifications. Genomic DNA was digested with HinfI. Following electrophoresis, the gel was dried under vacuum for 1 h at room temperature and then for 1 h at 50˚C in Church mix (0.25 M Na_2HPO_4 pH 7.2, 1 mM EDTA, 7 % SDS), pre-hybridized at 50 ˚C for 1 h in Church mix (0.25 M Na_2HPO_4 pH 7.2, 1 mM EDTA, 7 % SDS) and hybridized overnight at 50˚C with 5' radioactively-labeled $(AACCCT)_3$ oligonucleotide. After hybridization, the gel was washed three times with 4 x SSC at room temperature and once with 4 x SSC at 40˚C (30 min each wash), and exposed to PhosphoImager. Following G-overhang hybridization, the gel was denatured by incubation in 0.5 M NaOH and 1.5 M NaCl for 30 min, neutralized in 1.5 M NaCl and 0.5 M Tris–HCl pH 7.0 twice for 15 min, rinsed with H_2O, pre-hybridized, hybridized and washed as previously. . To determine the relative overhang signal, the signal intensity for each lane was determined before and after denaturation using Image J software. The native hybridization signal (corresponding to the overhang) was divided by the signal obtained after denaturation and normalized to the control (set to 1). These overhang values reflect the portion of single stranded overhang from the overall telomere length. To correct for the different telomere lengths, the native/denatured values were multiplied by the mean TRF values and then normalized to the control (noted MTL*Nat/Den).

CRISPR/Cas9-mediated Apollo gene correction. SV40-transformed hTERT-immortalized fibroblasts from P2 were co-transfected with the pSpCas9(BB)-2A-GFP (PX458) containing the gRNA sequence 5'-GATTGCAATTGGTGTTGTCT-3' and a 140 nucleotides long specific DNA matrix corresponding to the *Apollo/SNM1B* WT sequence surrounding the L142S mutation of P2. The DNA matrix also contained two additional silent mutations to avoid CRISP/Cas9 activity on the matrix after recombination.

Expression Vectors. The cDNAs encoding full-length and mutated versions of human *Apollo* were

amplified from cDNA of control and patients and cloned into a p3XFLAG-myc-CMV-26 expression vector (Sigma). The N terminus 3XFLAG-tagged WT and mutated Apollo expressing vectors were used to transfect 293T cells.

Sister chromatid exchange detection. Cells were incubated with BrdU (30 μM) for two doubling times before 1 h incubation with colcemid (0.1 μg/mL) followed by KCl 5.6 g/L hypotonic shock and fixation (methanol/acetic acid 3:1 (v:v)). When indicated cells were treated with mitomycin C (10^{-6} M) for 16 h before the addition of BrdU. Cells were dropped on glass slides with acetic acid for metaphase fixation. Slides were incubated as follows: 1X PBS 5 min, Hoechst 33258 (50 μg/mL in PBS) 5 min, 1X PBS 5 min, 2X SSC 1 min. Slides were incubated in 2X SSC were placed under UV light for 20 min. Slides were then mounted with DAPI (1/1000; 62248 thermofisher) and Fluorsave (345789, Merck Millipore).

Western Blotting and coimmunoprecipitation. Cells were lysed for 20 min on ice in 300 μL of lysis buffer (TNE) containing 50 mM Tris (pH 8.0), 2 mM EDTA, 0.5 % Nonidet P-40, 1 % phosphatase inhibitor cocktails (1 and 2, Sigma), and protease inhibitor (Roche Applied Science). One mg of cell lysate was incubated (1 h, 4 °C) with nonspecific IgG and 20 μL of prewashed magnetic beads (B23202 Bimake), beads were used as a negative control. Supernatant was then incubated with 2 μg of anti-FLAG (M2, F1804, Sigma) and 20 μL of prewashed magnetic beads. Immune complexes were collected with a magnetic separator and washed 5 times with lysis buffer. Immunoprecipitates were analyzed by Western blotting with murine monoclonal anti-FLAG (M2, F1804, Sigma) and anti-TRF2 (NB110-57130, Novus) and fluorescent secondary antibodies from LI-COR.

Sensitivity to genotoxics and complementation survival assay. Cellular sensitivity was performed by seeding cells at low density in complete culture medium and incubated with increasing doses of genotoxic drugs. After 7 days, surviving cells were either counted by using flow cytometry with a constant amount of fluorescent beads and survival fraction was calculated relative to untreated cells or by following the cellular growth via Incucyte® Systems for Live-Cell Imaging and Analysis (Zoom and S3; Sartorius).

Statistical Analyses. Statistical analyses were performed on Prism (GraphPad Software). For telomeric aberrations observed by FISH and chromosome anomalies, the two-sided probability values were obtained from a 2 × 2 contingency table analyzed using the Chi-square test. Telomeres of each condition were compared considering the total number of chromatid ends (because one chromosome may exhibit more than one telomere aberration). The number of chromatid fusion with telomeric material was considered (because one chromosome can fuse with one or more telomeric ends). For survival analysis groups were analyzed by two-tailed student t-test.

Supplemental references

1. Buck D, Malivert L, de Chasseval R, et al. Cernunnos, a novel nonhomologous end-joining factor, is mutated in human immunodeficiency with microcephaly. *Cell*. 2006;124(2):287-299.

2. Lesport E, Ferster A, Biver A, et al. Reduced recruitment of 53BP1 during interstrand crosslink repair is associated with genetically inherited attenuation of mitomycin C sensitivity in a family with Fanconi anemia. *Oncotarget*. 2018;9(3):3779-3793.

3. Gratia M, Rodero MP, Conrad C, et al. Bloom syndrome protein restrains innate immune sensing of micronuclei by cGAS. *J Exp Med*. 2019;216(5):1199-1213.

4. Lai TP, Zhang N, Noh J, et al. A method for measuring the distribution of the shortest telomeres in cells and tissues. *Nat Commun*. 2017;8(1):1356.

5. Awad A, Glousker G, Lamm N, et al. Full length RTEL1 is required for the elongation of the single-stranded telomeric overhang by telomerase. *Nucleic Acids Res*. 2020;48(13):7239-7251.

Supplementary Data

Supplementary Table 1. Hematological and immunological features of the patients.

Hematological features				
	P1	**P2**	**P3**	
Age at first evaluation	4 months	2 months	3 months	**Normal Values**
Blood count at first evaluation				
Total WBC (10^9/L)	**4.8**	**5.12**	8.77	6.0-17.5
PMN (10^9/L)	**0.6**	1.95	3.33	1.0-6.6
Lymphocytes (10^9/L)	**3.8**	**2.46**	4.9	4.0-10.6
Hemoglobin (g/dL)	10.9	**7.5**	**6.4**	9.5-13.5
Reticulocytes (10^9/L)	NA	48	NA	18-158
Platelets (10^9/L)	**13**	**19**	**81**	140-440
Age at start of transfusion support	10 months	2 months	3 months	
Immunological features				
	P1	**P2**	**P3**	
Age at evaluation	8 months	3 months	3 months	**Normal Values**
Lymphocyte counts at first evaluation				
Total count (/µL)	**2900**	**1650**	3460	3000-10600
CD3+ count (/µL)	2842	**1067**	3252	1900-5900
CD3+CD4+ (/µL)	1769	NA	2180	1400-4300
CD4+CD45RA+/CD4+ (%)	95	75	**96**	88-95
CD4+CD45RA+CD31+/CD4+ (%)	**40**	NA	**51**	60-72
CD3+CD8+ (/µL)	1015	NA	1073	500-1700
CCR7+CD45RA+/CD8+ (%)	88	NA	**10**	52-68
CCR7+CD45RA-/CD8+ (%)	**6**	NA	**1**	3-4
CCR7-CD45RA-/CD8+ (%)	**4**	NA	76	11-20
CCR7-CD45RA+/CD8+ (%)	**2**	NA	**13**	16-28
CD19+(/µL)	**12**	**3**	**173**	610-2600
CD3-CD56+CD16+ (/µL)	**14**	**6**	**31**	160-950
T cell function				
Proliferation to PHA	Normal	NA	Normal	
Proliferation to Antigens	Diminished to Tetanus toxoid Null for Candidin	NA	NA	
Ig levels at first evaluation				**Normal Values**
IgG (g/L)	3.51	5.83	**0.168**	1.64-5.88
IgA (g/L)	0.45	0.55	**<0.07**	0.07-0.66
IgM (g/L)	**<0.04**	0.26	**<0.04**	0.25-1.32
Serologic testing	NA	NA	NA	

NA: Not available; Ig: immunoglobulin; L: liter; g: gram; WBC: White blood cells; PHA: phytohemagglutinin; PMN: polymorphonuclear leukocyte.
Values out of the normal range are indicated in bold.
$CD3^+$ $CD4^+$ $CD45RA^+$ $CD31^+$ cells represent recent thymus emigrant T lymphocytes.
$CD3^+$ $CD8^+$ $CCR7^-$ $CD45RA^-$ cells represent central memory T cells.

Supplementary Table 2. Characterization of *Apollo* variants identified in individuals P1, P2 and P3.

Patient	Year of birth	Origin	Consanguinity	Variant status	Variant genomic	Variant cDNA	Variant protein	gnomAD freq.	CADD score	ACMG classification
Patient 1	2013	France	no	compound	Chr1:g.113908017C>T	c.364C>T	p.Arg122*	4.4e-5	39	Class 5 (PVS1, PS4, PM2, PM3, PP4)
				heterozygous	Chr1:g.114450701A>T	c.426A>T	p.Leu142Phe	0	28.5	Class 5 (PS4, PM1, PM2, PM3, PP3, PP4)
Patient 2	2009	Portugal	yes	homozygous	Chr1:g.114450700T>C	c.425T>C	p.Leu142Ser	0	25.5	Class 5 (PS4, PM1, PM2, PM3, PP3, PP4)
Patient 3	2014	Argentina	no	compound	Chr1:g.114450747C>T	c.472C>T	p.Arg158*	3.18e-5	38	Class 5 (PVS1, PS4, PM2, PM3, PP4)
				heterozygous	Chr1:g.114450700T>C	c.425T>C	p.Leu142Ser	0	25.5	Class 5 (PS4, PM1, PM2, PM3, PP3, PP4)

ACMG classification as described in Richards et al. [1]
gnomAD database version V2.1.11

Supplementary Figure 1

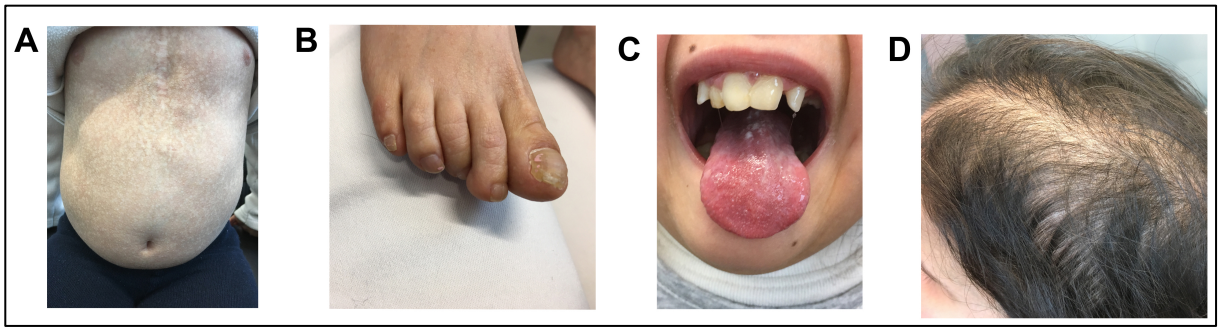

Supplementary Figure 1: Mucocutaneous features in patient P2. P2 exhibited the mucocutaneous anomalies of dyskeratosis congenita [2-4], including abnormal pigmentation of the trunk (**A**), dystrophic nails (**B**), leukoplakia (**C**), and sparse scalp hair (**D**).

Supplementary Figure 2

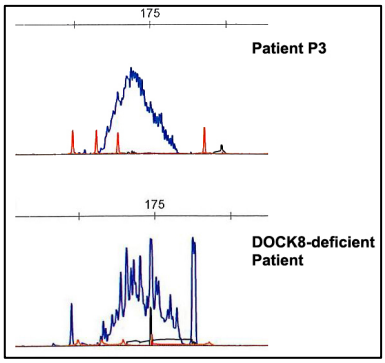

Supplementary Figure 2. T cell repertoire in patient P3. Analysis of T-cell Receptor Gamma (TRG) rearrangements by multiplex PCR indicated that patient P3 did not exhibit bias in T cell repertoire and clonality [5]. Sample from a DOCK8-deficient patient was used as a control of TRG clonality.

Supplementary Figure 3

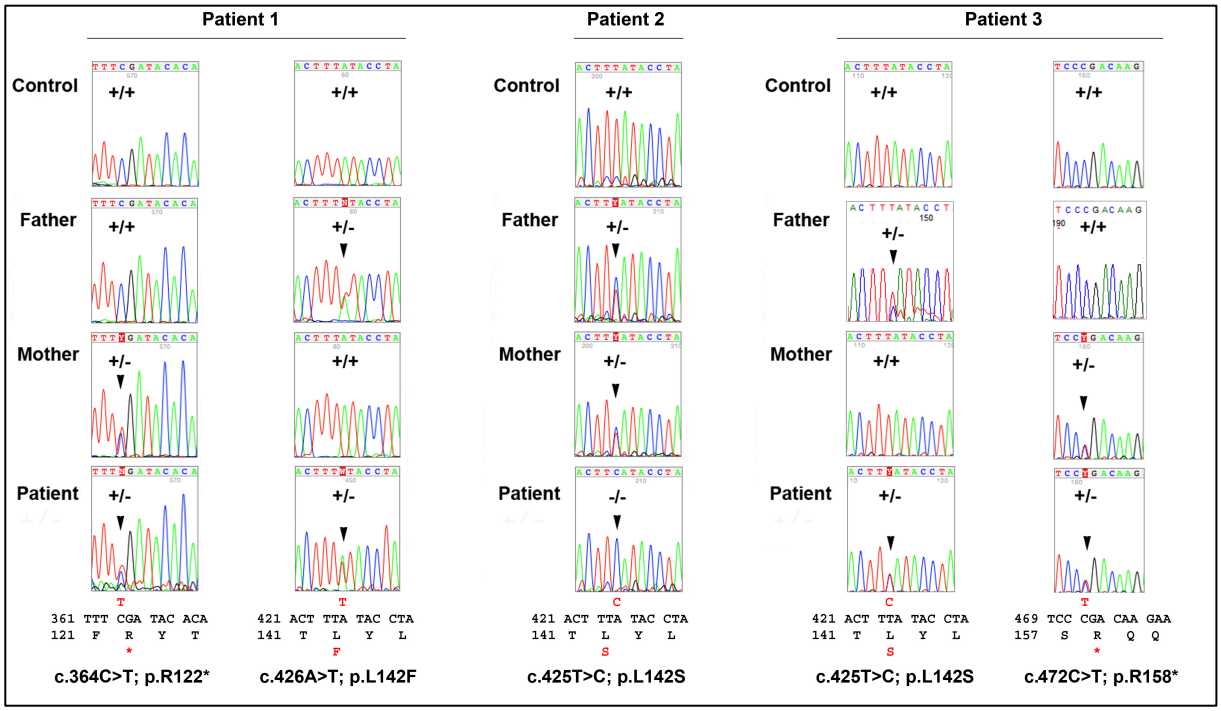

Supplementary Figure 3. Inheritance of *Apollo* variants detected in P1, P2, and P3. Direct Sanger sequencing of Apollo variants in a healthy control, in patients P1, P2, P3 and their parents. The red letters indicate the nucleotide changes (above) and the amino-acid residue modification (below) relative to the WT sequence.

Supplementary Figure 4

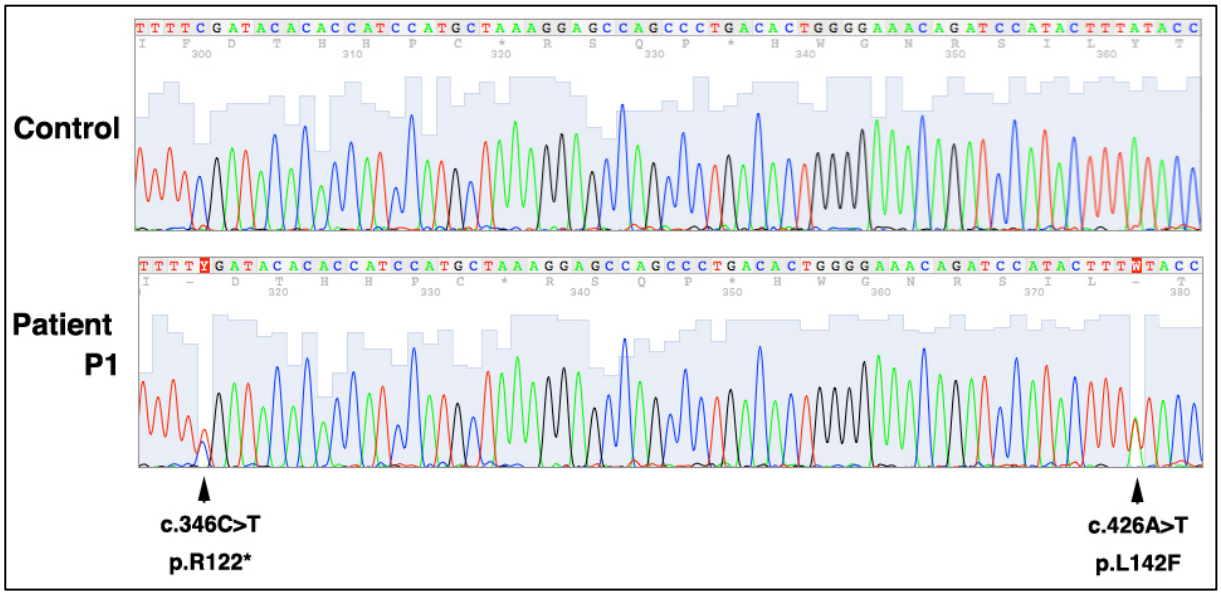

Supplementary Figure 4. The c.346C>T; p.R122* *Apollo* variant does not cause nonsense-mediated decay (NMD). Direct sequencing of *Apollo* cDNA from P1's fibroblasts similarly detected the c.346C>T; p.R122* variant and the c.426A>T, p.L142F variant. This result indicates that the c.346C>T; p.R122* variant does not cause nonsense-mediated decay NMD.

Supplementary Figure 5

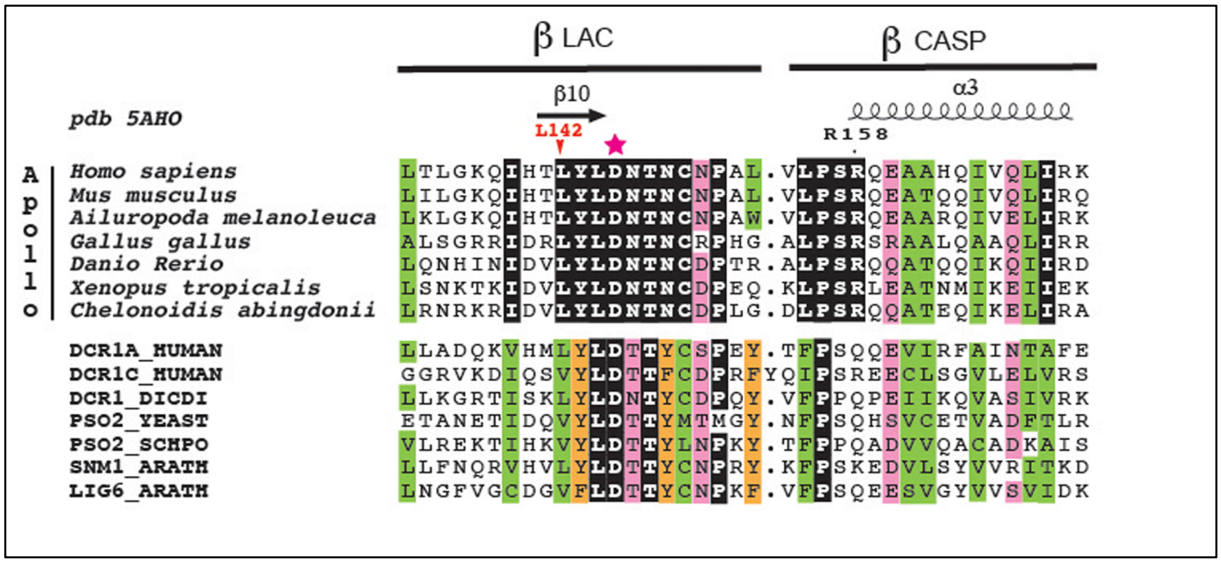

Supplementary Figure 5. Sequence alignment of human Apollo with representative orthologs and other members of the beta-CASP family (UniProt Entry names)**.** A red arrow highlights the residue L142. The pink star corresponds to the conserved D145 residue.

Supplementary Figure 6

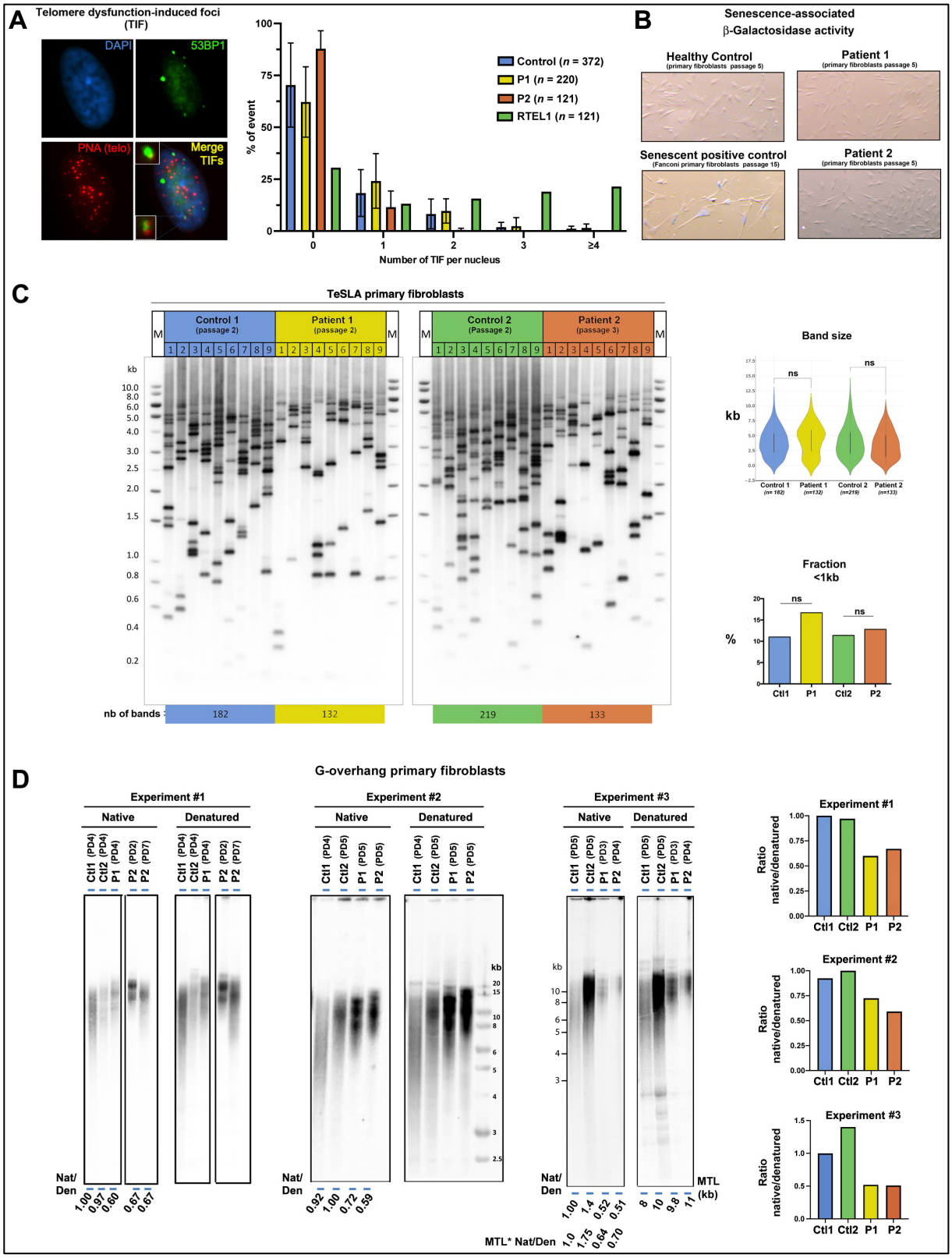

Supplementary Figure 6. Telomere phenotype in patients' primary fibroblasts. (**A**) (Up) Detection of telomere dysfunction-induced foci (TIF) by the colocalization of telomeric FISH signal (PNA) with the DNA repair factor 53BP1. (Down) Quantitative analysis of TIFs in primary fibroblasts from a

healthy control (passage numbers 4-7), the patients P1 (passage numbers 3 and 4) and P2 (passage numbers 2-4). Primary fibroblasts from an RTEL1-deficient patient (P1 in Le Guen et al.[6]) were used as TIFs positive control (passage number 3). Numbers of nuclei counted are indicated. Results obtained from at least two independent experiments (except for RTEL1 deficient cells; *n* = 1). (**B**) Detection of senescent cells by senescence-associated β-galactosidase activity. Passage numbers are indicated. (**C**) (Left) Detection of the shortest telomeres by TeSLA performed in primary fibroblasts from two age-matched healthy donors and the two patients P1 and P2. (Right) Graphic representation of TeSLA results. Statistical analyses are represented. A two-tailed student t-test was used for statistical analyses of band size and a χ2 test was used for analysis of fraction <1kb. (**D**) (Left) Measurement of G-overhang signal by native versus denatured in-gel hybridization method with a C-rich telomeric probe in three independent experiments with DNA from controls and patients' primary fibroblasts at the indicated population doublings (PD). The G-overhang (native) signals were normalized to the corresponding denatured signals and then to one of the controls in each gel. Values after correction for the effect of the telomere length (noted MTL*Nat/den) are shown in experiment #3. (Right) Graphical representation of G-overhang results.

Supplementary Figure 7

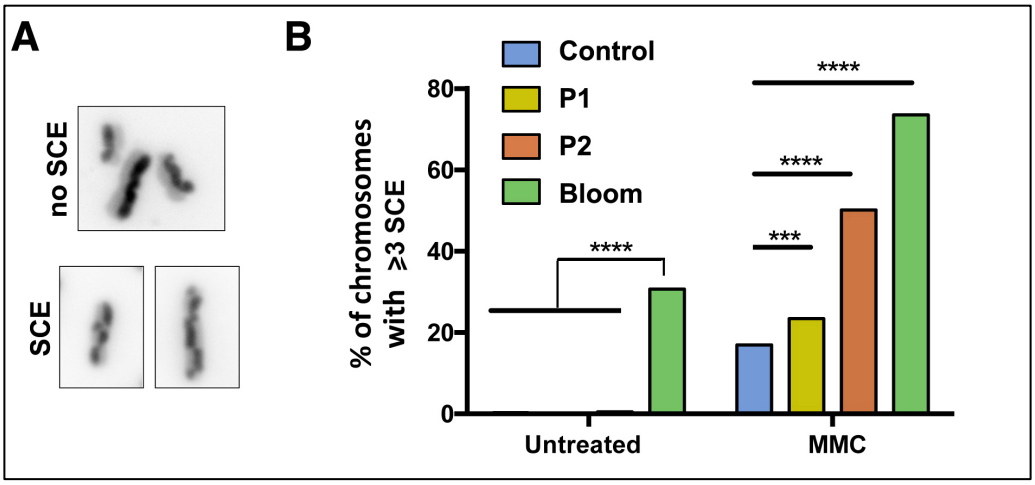

Suppl. Figure 7. Increased MMC-induced sister chromatid exchanges (SCE) in patients' cells. Representative pictures of chromosome without and with SCE. (**E**) Quantitative analysis of SCE in untreated and MMC-treated cells. Cells from a Bloom-deficient patient are used as a positive control. Results representative of 3 independent experiments without MMC and 1 experiment with MMC. (Counted chromosomes: Ctrl -MMC: *n* = 647; Ctl +MMC: *n* = 413; P1 -MMC: *n* = 1,298 P1 +MMC: *n* = 516; P2 -MMC: *n* = 2242; P2 +MMC: *n* = 361; Bloom -MMC: *n* = 114; Bloom +MMC: *n* = 87). Averages are shown and chi-square tests were applied to compare Ctl with P1, P2, and Bloom.

Supplementary Figure 8

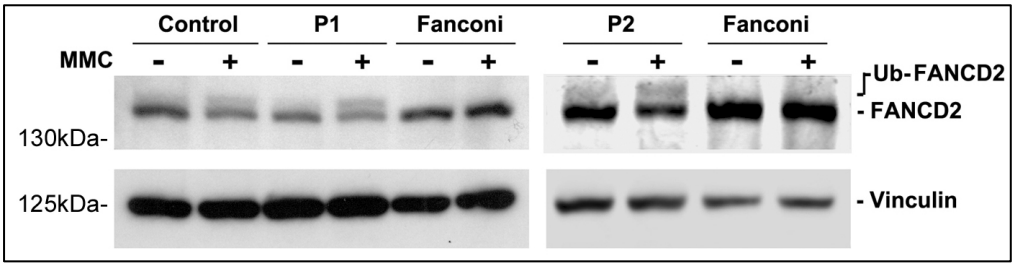

Suppl. Figure 8. Detection of FANCD2 ubiquitination in MMC-treated patients' cells. Detection of FANCD2 ubiquitination by Western blot after MMC treatment (150 ng/mL for 48 h) of fibroblasts from patients P1 and P2, a healthy control, and a Fanconi anemia patient (used as negative control). Vinculin is used a loading control.

Supplementary Figure 9

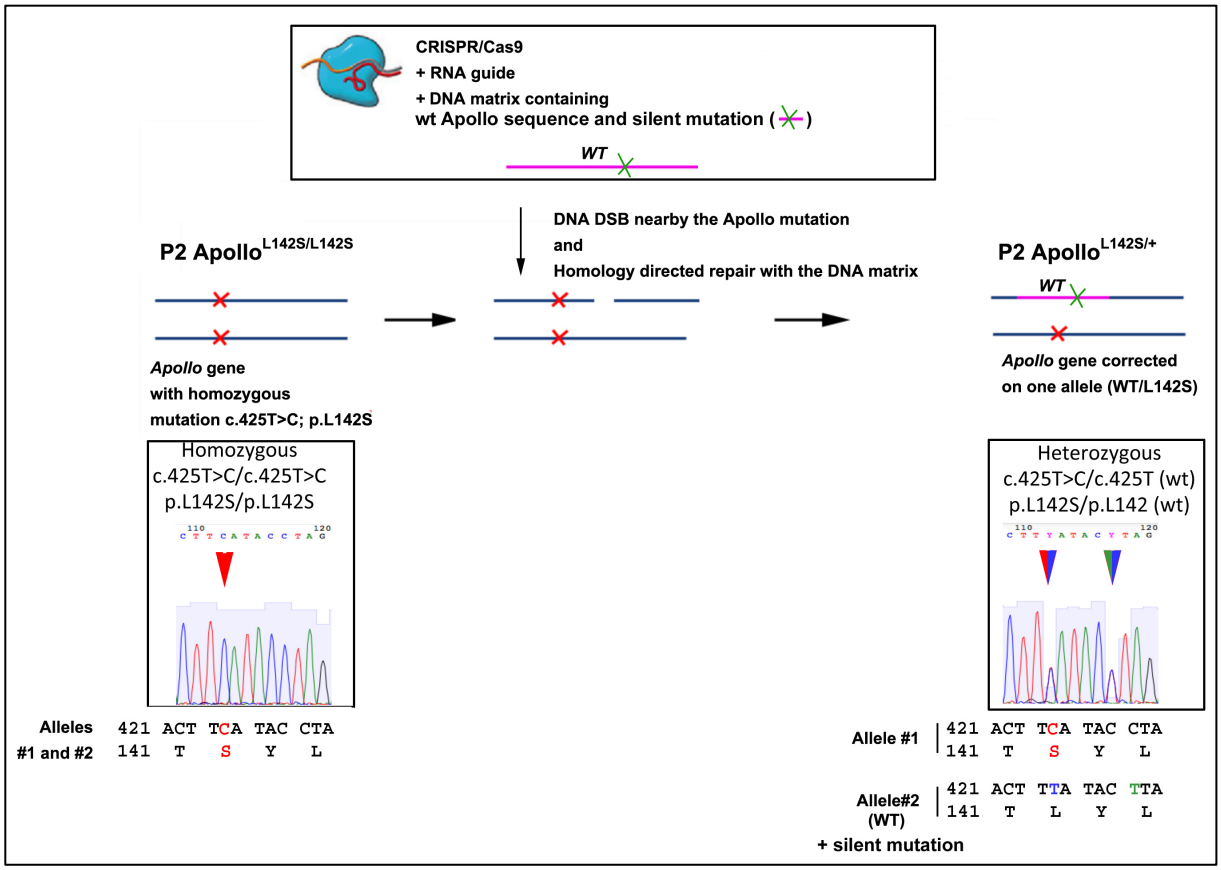

Supplementary Figure 9. *Apollo* gene correction in one allele mediated by CRISPR/Cas9 in P2's cells. (Up) Schematic representation of *Apollo* gene correction mediated by CRISPR/Cas9 in P2's cells. (Down) Direct Sanger sequencing of P2's cells before and after gene correction indicates that one Apollo allele recombined with the DNA matrix carrying WT Apollo sequence (blue/red arrow) and a silent mutation (blue/green arrow).

Supplementary Figure 10

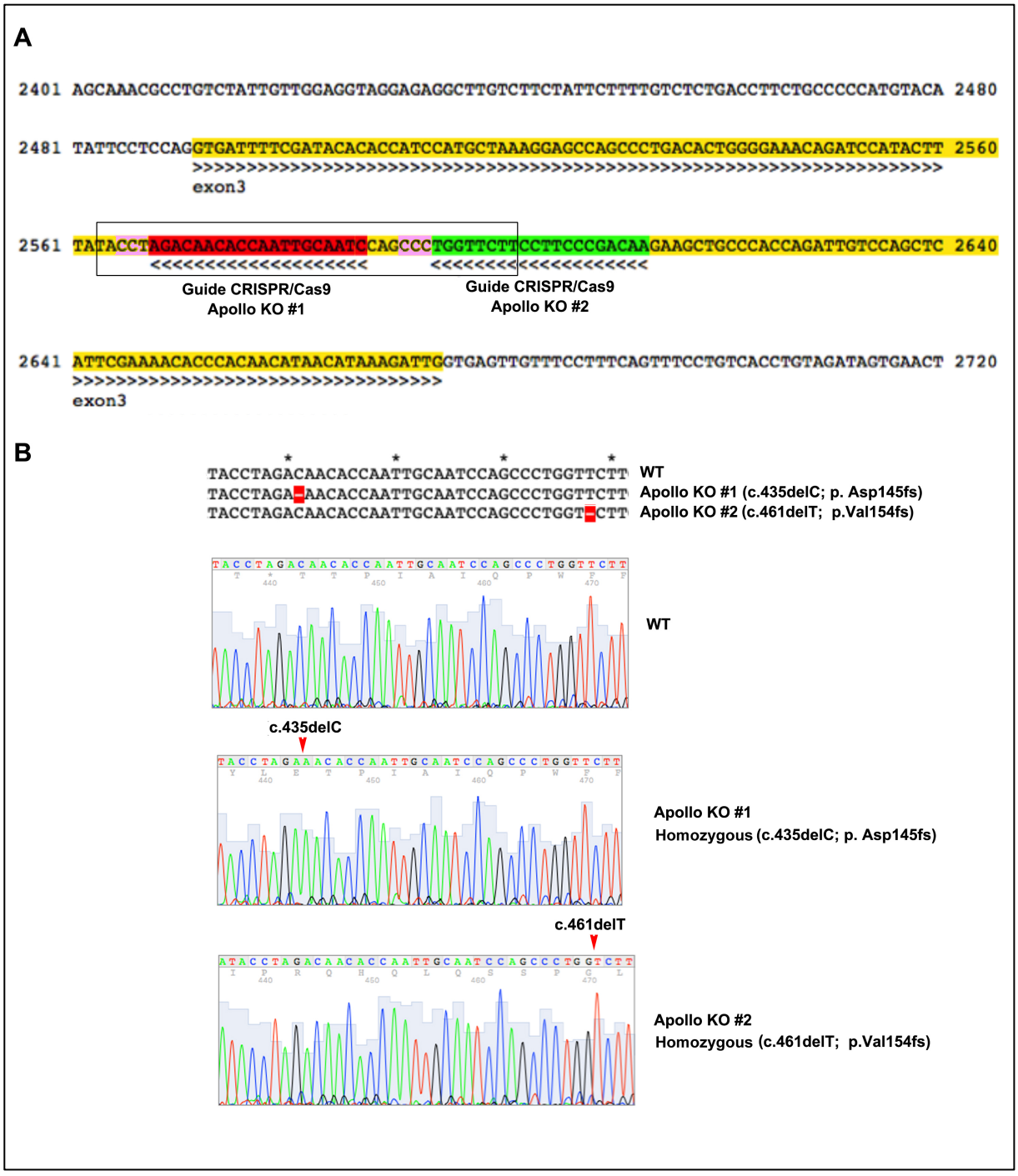

Suppl. Figure 10. **Generation of Apollo KO HT1080 cell lines.** (**A**) Design of the two guide RNAs (#1 and #2) used to create CRISPR/Cas9 mutations in the Apollo coding sequence (exon 3 in yellow). Box represents the sequence depicted in (B). The red and green sequences represent the loci targeted by the gRNA #1 and #2, respectively. The pink sequences represent the PAM. (**B**) The HT1080 Apollo KO clone #1, generated with the gRNA#1, harbors a homozygous 1-bp deletion c.435delC resulting in a frameshift and a premature stop codon. The HT1080 Apollo KO clone #2, generated with the gRNA#2, harbors a homozygous 1-bp deletion c.461delT leading to a frameshift and a premature stop codon.

References

1. Richards S, Aziz N, Bale S, et al. Standards and guidelines for the interpretation of sequence variants: a joint consensus recommendation of the American College of Medical Genetics and Genomics and the Association for Molecular Pathology. *Genet Med*. 2015;17(5):405-424.
2. Armanios M, Blackburn EH. The telomere syndromes. *Nat Rev Genet*. 2012;13(10):693-704.
3. Savage SA. Beginning at the ends: telomeres and human disease. *F1000Res*. 2018;7.
4. Calado RT, Young NS. Telomere diseases. *N Engl J Med*. 2009;361(24):2353-2365.
5. Armand M, Derrieux C, Beldjord K, et al. A New and Simple TRG Multiplex PCR Assay for Assessment of T-cell Clonality: A Comparative Study from the EuroClonality Consortium. *Hemasphere*. 2019;3(3):e255.
6. Le Guen T, Jullien L, Touzot F, et al. Human RTEL1 deficiency causes Hoyeraal-Hreidarsson syndrome with short telomeres and genome instability. *Hum Mol Genet*. 2013;22(16):3239-3249.